

4-Methoxyanilinium Perrhenate 18-Crown-6: A New Ferroelectric with Order Originating in Swinglike Motion Slowing Down

Da-Wei Fu,¹ Hong-Ling Cai,^{1,3} Shen-Hui Li,² Qiong Ye,¹ Lei Zhou,² Wen Zhang,¹ Yi Zhang,¹
Feng Deng,² and Ren-Gen Xiong^{1,*}

¹Ordered Matter Science Research Center, Southeast University, Nanjing 211189, People's Republic of China

²State Key Laboratory Magnetic Resonance and Atomic Molecular Physics Wuhan Center for Magnetic Resonance, Wuhan Institute of Physics and Mathematics, Chinese Academy of Sciences, Wuhan 430071, People's Republic of China

³Department of Physics, Laboratory of Solid State Microstructures, Nanjing University, Nanjing 210093, China

(Received 8 October 2012; published 20 June 2013)

A supramolecular adduct 4-methoxyanilinium perrhenate 18-crown-6 was synthesized, which undergoes a disorder-order structural phase transition at about 153 K (T_c) due to slowing down of a pendulumlike motion of the 4-methoxyanilinium group upon cooling. Ferroelectric hysteresis loop measurements give a spontaneous polarization of $1.2 \mu\text{C}/\text{cm}^2$. Temperature-dependent solid-state nuclear magnetic resonance measurements reveal three kinds of molecular motions existing in the compound: pendulumlike swing of 4-methoxyanilinium cation, rotation of 18-crown-6 ring, and rotation of the methoxyl group. When the temperature decreases, the first two motions are frozen at about 153 K and the methoxyl group becomes rigid at around 126 K. The slowing down or freezing of pendulumlike motion of the cation triggered by temperature decreasing corresponds to the centrosymmetric-to-noncentrosymmetric arrangement of the compound, resulting in the formation of ferroelectricity.

DOI: [10.1103/PhysRevLett.110.257601](https://doi.org/10.1103/PhysRevLett.110.257601)

PACS numbers: 77.84.Fa, 61.50.Ks, 65.40.Ba, 82.56.-b

Ferroelectrics, as pyroelectric materials with reversal polarization, are widely used as electric-optical devices, information storages, switchable nonlinear optical devices, and light modulators [1]. Generally, the high-temperature phase of order-disorder-type ferroelectrics exhibits some kinds of orientational or positional disorders, whereas atomic or molecular motion accompanies large deformations and/or distortions of the atomic coordinates [2]. Decreasing temperature reduces thermal fluctuation of atomic motion, which results in structural phase transitions from a centrosymmetric atomic coordinate to a noncentrosymmetric one [3]. As a result, one effective method to obtain order-disorder type ferroelectrics is to design and construct crystals containing molecular motions [4]. Recently, we discovered a new ferroelectric, diisopropylammonium bromide, which has spontaneous polarization as large as that of BaTiO_3 and above room temperature transition temperature [5]. The surprisingly strong ferroelectric behavior in this organic compound suggests a reconsideration of the generality of charge interactions that underlie related properties [6]. Furthermore, Liu *et al.* [7] discovered ferroelectricity in biological materials, although piezoelectric and pyroelectric behaviors have been widely studied, which hints ferroelectric coupling is an important part of some biological processes [6]. Therefore, organic and/or organic-inorganic hybrid ferroelectric research [8] is very important since it acts as a bridge to the understanding of coupling in oxides and that in complex soft materials. However, because the crystal classes of ferroelectrics should be polar, materials including Buckminster fullerene, adamantane, cubane,

and hexamethylenetetramine, which undergo very fast reorientations and rotations in their high-temperature phases, are not good candidates for ferroelectrics because their rotations are along multiple rotational axes with very low rotation barriers [9].

Artificial molecular machines, in which molecules and/or ions appear to be loosely bound to the rest of the structure to realize unidirectional motions, have been recognized as appealing analogies between the structure of certain organic molecules and those of some machines and machine parts by chemists over the last two decades [10]. Among them, molecular rotators possessing a dipole-functionalized rotation, so-called molecular compasses, will provide opportunities for the dipole inversion. For instance, Akutagawa *et al.* reported that a supramolecular rotator exhibited dipole rotation resulting in a ferroelectric transition [11]. The supramolecular charge-transfer networks utilized a structural synergy between a hydrogen-bonded network and charge-transfer complexation of donor and acceptor molecules that reveal ferroelectric polarization switching with a high Curie temperature [12]. Kagawa *et al.* reported magnetically controllable ferroelectricity was realized in supramolecule tetrathiafulvalene-*p*-bromanil as the spin-Peierls instability [13]. Herein, as systematic works to investigate novel molecule-based ferroelectrics [5,14–20], we report ferroelectric properties of a supramolecular compound, 4-methoxyanilinium perrhenate 18-crown-6 (MOAP), in which the $-\text{NH}_3^+$ group of the 4-methoxyanilinium cation is fixed by strong hydrogen-bond interactions with oxygen atoms of the 18-crown-6, while the 4-methoxyphenyl

group acts as a directed-pendulum unit, resulting in a paraelectric-ferroelectric phase transition.

The crystal structure of MOAP [Figs. 1(a) and 1(b)] remains an orthorhombic crystal system while crystal symmetry transforms from a centrosymmetric space group of $Pnma$ to a noncentrosymmetric one of $Pna2_1$ [Fig. 1(c)] with an Aizu notation of $mmmFmm2$. The supramolecular cation is formed by a protonated 4-methoxyanilinium cation and 18-crown ether through strong hydrogen bond interactions between oxygen atoms of the 18-crown-6 ether and hydrogen atoms of the $-NH_3^+$ group in 4-methoxyanilinium cation. The NH_3^+ group is fixed in the cavity of the 18-crown-6 to form a rotator-stator assembly. Although the NH_3^+ group almost fixes in the center cavity of the 18-crown-6 ether with distance of 0.8657(9) Å between the NH_3^+ group and the center of 18-crown-6, the cation above the Curie temperature is disordered and shows two occupations: two phenyl rings lie in the same plane [Fig. 1(a)]. Therefore, the whole cation looks like a pendulum and swings from side to side in the phenyl ring plane.

The crystal structure at 93 K was measured in order to investigate whether the disordered cation is related to the motion of molecule or ion. Although the lattice parameters at 93 K are almost the same as those at 293 K (see Supplemental Material [21]), the mirror symmetry in the (010) plane is lost and a noncentrosymmetric space group $Pna2_1$ is adopted for the low-temperature structure [Fig. 1(b)]. The thermal vibration parameters of all atoms at 93 K are obviously smaller than those found at 293 K,

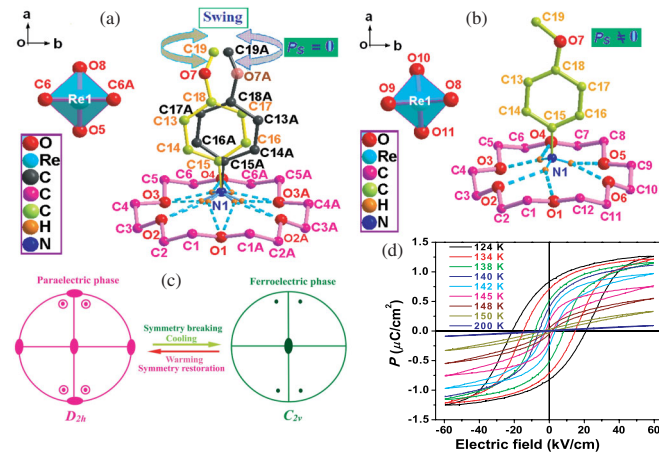


FIG. 1 (color online). Structural unit of MOAP in (a) the high-temperature phase (293 K, paraelectric phase) showing totally disordered 4-methoxyanilinium cation, and (b) the low-temperature phase (93 K, ferroelectric phase) showing ordered 4-methoxyanilinium cation. (c) shows the transformation of the point group of MOAP from high-temperature paraelectric phase ($Pnma$ with symmetric elements: $E, C_2, C_2', C_2'', i, \sigma_h, \sigma_v, \sigma_v'$) to low-temperature ferroelectric phase ($Pna2_1$ with symmetric elements: $E, C_2, \sigma_v, \sigma_v'$). (d) Dielectric hysteresis loops of MOAP recorded along the c axis measured at frequency of 50 Hz and different temperatures.

which means the motions of all molecules are almost frozen. The disordered 4-methoxyanilinium cation turns from disorder to order with the temperature decreasing.

Temperature-dependent second harmonic generation (SHG) is very sensitive to occurrence of symmetry breaking [5,14]. The result that the space group of MOAP turns from centrosymmetric $Pnma$ to noncentrosymmetric $Pna2_1$ as temperature decreasing according to the single-crystal structure determination was confirmed by SHG as shown in Fig. 2(a). There is almost no signal at 532 nm above 153 K. A clear peak appears below 153 K, indicating that the structure of MOAP changes from a centrosymmetric structure to a noncentrosymmetric one, which is consistent with XRD structure analysis.

Differential scanning calorimetry (DSC) measurement, which is a good method to confirm whether a sample undergoes a phase transition or not, shows anomalies at about 151 K (cooling) and 153 K (heating) [Fig. 2(b)]. The entropy change ΔS is equal to about $3.25 \text{ J} \cdot \text{mol}^{-1} \cdot \text{K}^{-1}$ ($\approx R \ln 3/2$). The shape of the heating flow, the thermal hysteresis ($\sim 2 \text{ K}$), and the entropy change (ΔS) suggest the phase transition is of an order-disorder type. Specific heat capacity measurement reveals a characteristic anomaly at around 153 K [Fig. 2(b)]. The entropy change ΔS connected with the anomaly is estimated to be $3.05 \text{ J} \cdot \text{mol}^{-1} \cdot \text{K}^{-1}$. The characteristic anomaly is observed at 153 K and the round shape of the anomaly peak most likely resembles the features of a second-order phase transition.

Generally, strong anomalies in dielectric, elastic, and other physical properties accompany with the paraelectric-ferroelectric structural phase transition [22].

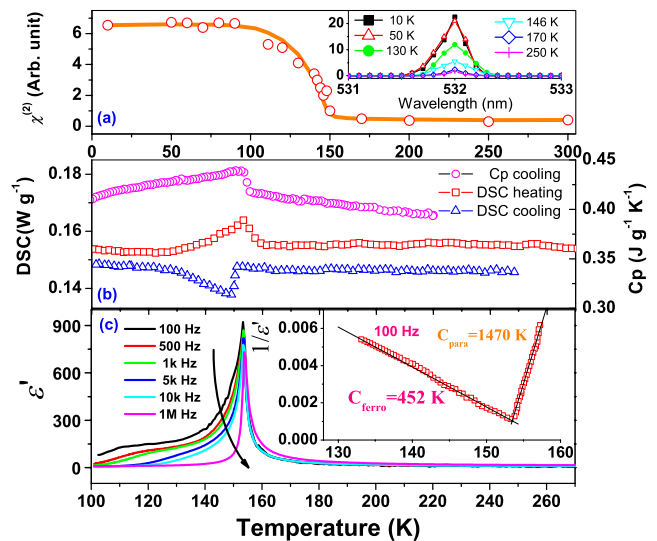


FIG. 2 (color online). (a) Temperature dependence of the second-order nonlinear optical coefficient. The inset shows the wavelength dependence of SHG intensity at different temperatures. (b) Temperature dependence of heat capacity (C_p) and DSC obtained on a heating-cooling cycle. (c) Temperature dependence of dielectric constant at different frequencies. The inset shows the Curie-Weiss law fitting of the dielectric constant at a frequency of 100 Hz in the interval of phase transition.

Moreover, molecular motions in crystals are often responsible for the dielectric response [23]. Figure 2(c) shows the real part of temperature-dependent dielectric constant (ϵ') of MOAP along the c axis at different frequencies. It is interesting to note that a strong anomaly or a sharp peak appears around $T_c = 153$ K. At the highest frequency, the dielectric temperature dependence is typical of a continuous paraelectric-ferroelectric phase transition and the dielectric constants turn from 10 to 770 at T_c with a $77\times$ increase. The inset plot of Fig. 2(c) is the reciprocal of dielectric constant versus temperature at 100 Hz. It is linear and continuous near the Curie point. According to the Curie-Weiss law, $\epsilon = \epsilon_\infty + C/(T - T_c)$, the fitted Curie-Weiss constants C_{para} of the paraelectric phase and C_{ferro} of the ferroelectric phase are comparable to those found in the typical order-disorder type ferroelectrics, such as colemanite, NH_4HSO_4 , $(\text{NH}_2\text{CH}_2\text{COOH})_2\text{HNO}_3$, and $(\text{CH}_3\text{NH}_3)\text{Al}(\text{SO}_4)_2 \cdot 12\text{H}_2\text{O}$. The ratio of $C_{\text{para}}/C_{\text{ferro}}$ is 3.2 at the lowest frequency, larger than 2 and approximate to 4, and is characteristic of the second-order ferroelectric transition. For the origin of the dielectric anomaly, non-polar change accompanied with the rotation of 18-crown-6 will not result in the dielectric anomaly. The sharp peak and the strong dielectric anomalies at T_c should be attributed to the pendulumlike motion of the 4-methoxyanilinium cation. Since low frequency dielectric properties are more sensitive to the molecular motion, the shoulder peak at around 120 K at low frequencies is attributed to the forward-backward motion of the methoxyl group.

The electric hysteresis loops of MOAP along the polar c axis at different temperature are recorded on a Sawyer-Tower circuit at 50 Hz as shown in Fig. 1(d). The maximum electric field E_{max} is about $21.4 \text{ kV} \cdot \text{cm}^{-1}$. The loop is a straight line at 200 K as a paraelectric phase. With the temperature decreasing to ferroelectric phase temperature range, a typical ferroelectric loop appears at about 150 K which is below the T_c . Upon further cooling, the ferroelectric loop reaches saturation at about 124 K with a spontaneous polarization of about $1.2 \mu\text{C} \cdot \text{cm}^{-2}$ and a remanent polarization of $0.9 \mu\text{C} \cdot \text{cm}^{-2}$, which is obviously larger than those found in Rochelle salt ($0.2 \mu\text{C} \cdot \text{cm}^{-2}$), ammonium sulfate ($0.25 \mu\text{C} \cdot \text{cm}^{-2}$), dicalcium strontium propionate ($0.30 \mu\text{C} \cdot \text{cm}^{-2}$) and guanidinium aluminum sulfate hexahydrate ($0.35 \mu\text{C} \cdot \text{cm}^{-2}$), but significantly smaller than that of triglycine sulfate ($3.5 \mu\text{C} \cdot \text{cm}^{-2}$).

As mentioned above, three kinds of motion, including the pendulumlike motion of 4-methoxyanilinium, rotation of 18-crown-6, and forward-backward motion of methoxyl group, coexist in MOAP in the high-temperature paraelectric phase. Temperature-dependent solid-state nuclear magnetic resonance (NMR) measurement was used to detect the molecular motions in MOAP in order to explore the origin of ferroelectricity as shown in Fig. 3, in which the labels of each atom are consistent with those highlighted in Fig. 1(b). The chemical shifts at 57 ppm can be

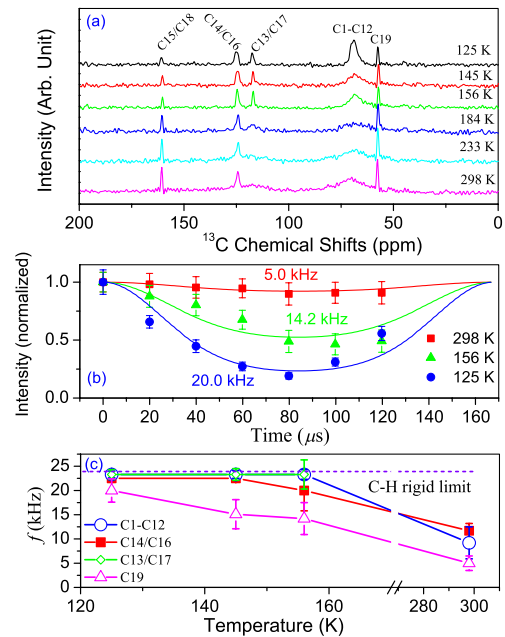


FIG. 3 (color online). (a) ^{13}C MAS NMR spectra of MOAP acquired at different temperatures. (b) ^{13}C - ^1H dipolar couplings of methoxy C19 measured at different temperatures. The dipolar dephasing curves are extracted from the t_1 dimension of 2D DIPSHIFT spectra. The true coupling strengths, which were calculated from the simulated values and scaling factor, are indicated. (c) The temperature dependence of dipolar coupling for these nonquaternary carbon atoms.

assigned to terminal methoxy species (C19). The resonance at around 69 ppm arises from the 18-crown-6 (C1-C12). Additionally, the peaks at 160, 125, and 117 ppm are due to the aromatic carbon atoms C18/C15, C14/C16, C13/C17 in the phenyl ring of the 4-methoxyanilinium cation, respectively.

In the temperature range 298–184 K, the linewidths of C14/C16 and C15/C18 aromatic sites are relatively narrow, whereas those of C13/C17 aromatic sites are much broader and almost undetectable. The low sensitivity of C13/C17 sites might be associated with an intermediate motion of these sites, in analogy to other biological systems [24]. It is noteworthy that the chemical environments of C14/C16 and C13/C17 sites are quite similar. The variation difference of their linewidths in the temperature range 298–184 K is ascribed to the difference of regional motions among these aromatic carbon sites in the phenyl ring. Based on the NMR observations, we deduce that the aromatic ring in 4-methoxyanilinium is likely in a motion mode of pendulumlike swing rather than a phenyl rotation. The swing of phenyl ring enables the motion amplitude of C13/C17 greater than that of C14/C16 sites. It is interesting to note that the linewidth of aromatic C13/C17 sites is dramatically narrowed at 156 K, indicating that the swing of the phenyl ring is frozen at that temperature. These results are consistent with the analysis of single crystal structure (Fig. 1). The linewidth variation of C1–C12 sites in the 18-crown-6 ring is quite similar to that of C13/C17

sites in the phenyl ring, indicating the presence of intermediate motion of 18-crown-6 above 156 K. The linewidth of C1-C12 sites decreases dramatically as the temperature reaches 156 K, suggesting that the 18-crown-6 might become rigid at 156 K. Further decreasing the temperature, the peak becomes more and more sharp. The linewidth variation is probably associated with the disorder-order transition at around 156 K for MOAP.

To obtain more quantitative information on the motional amplitude to reflect the dynamics behavior of MOAP, we used a 2D dipolar chemical shift correlation (DIPSHIFT) experiment to yield the one-bond C-H coupling strength as well as order parameters [25]. In DIPSHIFT experiments, one-bond C-H coupling strength relative to rigid limit (23.9 kHz) [26,27] can directly manifest the regional molecular motion. Figure 3(b) shows the ^{13}C - ^1H dipolar couplings frequency for methoxyl C19 sites obtained from DIPSHIFT experiments at different temperatures. The C-H dipole coupling strength in these carbon sites at different temperatures was shown in Fig. 3(c). For example, the one-bond C-H dipole coupling in C14/C16 sites is determined to be 11.7 ± 1.5 kHz at room temperature. Accordingly, the order parameter of the C14/C16 sites, which reflects the motion of phenyl ring, is determined to be around 0.52, confirming the presence of segmental motion of phenyl ring at room temperature. The coupling strength of C19 at room temperature is 5 ± 1.5 kHz, corresponding an order parameter of 0.22, which is the smallest value for all the carbon sites, revealing the high flexibility of the methoxyl group. The coupling strength decreases with decreasing temperature [Fig. 3(c)]. At 145 K, the one-bond ^{13}C - ^1H dipole couplings for C14/C16, C13/C17, and C1-C12 sites are measured to be 22.5 ± 0.5 , 23.3 ± 1.2 , and 23.3 ± 0.8 kHz, respectively, very close the C-H rigid limit value (23.9 kHz). Accordingly, the order parameters of the C14/C16, C13/C17, and C1-C12 sites are calculated to be 0.94, 0.97, and 0.97, respectively, indicating that both phenyl motion and regional motion of 18-crown-6 are frozen and sample MOAP has been rigid at 145 K. Interestingly, the segmental motion of the methoxyl group is not completely restricted at 156 K, in which the torsional libration motion instead of the three-site jump is still present. Moreover, it is revealed the terminal methoxyl group becomes considerably rigid as the temperature decreases to 125 K.

The ordered-disordered orientation changes of the cation have been observed in the low- and high-temperature phases. Meanwhile, the pendulumlike motion of the cation and dynamic behavior of the terminal methoxyl species has been verified by solid-state NMR measurement. Herein we evaluate the potential energies for the pendulumlike motion of the cation, rotation of the phenyl and methoxyl groups by using the restricted Hartree-Fock calculation method, and the atomic coordinates at 93 K. The basic set of Re atom is LanL2DZ while for other atoms the basic set is 6-31G(d) [28].

According to the results of disordered high-temperature phase and solid-state NMR measurement, i.e., the motion amplitude of C13/C17 is greater than that of C14/C16 sites, we first evaluate the pendulumlike motion of the whole cation on the plane of phenyl ring with fixed $-\text{NH}_3^+$ group in the crown ether center. The initial atomic coordinates from the x-ray crystal structural analyses at 93 K corresponded to the first potential energy minimum at the $\phi = 0^\circ$, whose relative energy is defined as zero. An asymmetric potential energy profile is observed for pendulumlike motion of the whole cation [Fig. 4(a)]. The pendulumlike motion is mainly restricted by the nearest-neighbor ReO $_4^-$ anions and two other cations in this region. ΔE values less than $100 \text{ kJ} \cdot \text{mol}^{-1}$ are observed for the pendulumlike motion in the range $-10^\circ < \phi_1 < +10^\circ$, which indicates that the pendulumlike motion of the cation is thermally activated at 300 K in the motion range $-10^\circ < \phi_1 < +10^\circ$. Such motion may be frozen at lower temperatures due to the decrease in thermal energy as found in solid-state NMR measurement results. Therefore, the origin of ferroelectricity can be understood as the pendulum is swinging in a double-minimum potential well, and the transition occurs when these cations collectively freeze into one of these two wells.

The rigid rotation energies of phenyl and methoxyl groups are also evaluated. For the rotation of the phenyl group along the C-N axis (ϕ_2), the atomic coordinates of the $-\text{NH}_3^+$ and $-\text{OMe}$ groups are fixed and rigid rotation of the phenyl ring is applied for the rotation angle dependence.

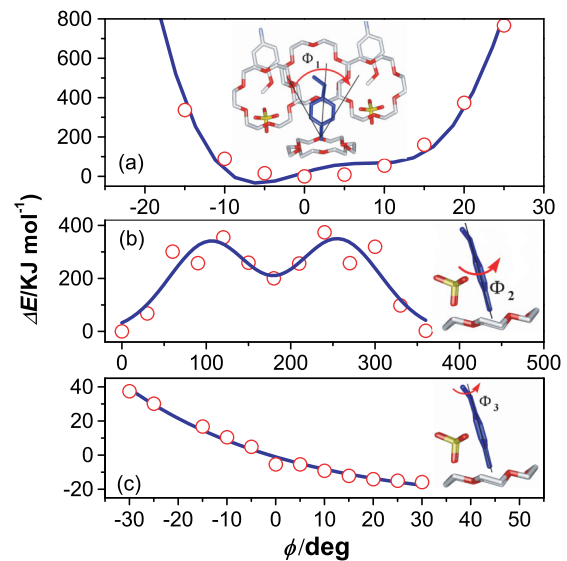


FIG. 4 (color online). Potential energy calculations for (a) pendulumlike motion of the cation, (b) the phenyl group rotation, and (c) rotation of the methoxyl group, where the solid lines are fitting lines to the data. The insets show the initial structure for the calculation: (a) the cation moves on the benzene ring plane by fixing the NH_3^+ group in the crown ether ring center; (b) the rotation along C-N axis with fixed NH_3^+ moiety and methoxyl group; (c) the rotation along C-O axis with fixed NH_3^+ and phenyl groups.

The almost symmetric calculation double-minimum type potential energy curves are observed in rotation potential energies of phenyl ring as shown in Fig. 4(b). The second energy minimums are observed at 180° . The potential energy barriers ΔE of the phenyl group rotation are about $350 \text{ kJ} \cdot \text{mol}^{-1}$ observed at $\phi_2 = 90^\circ$ and 270° . Such a large rotation energy barrier means the rotation of the phenyl group is difficult even at room temperature, which dovetails with that found in solid-state NMR measurements. Since the 360° rotation of the methoxyl group (ϕ_3) should be impossible due to the large steric hindrance of the neighboring crown ethers, anions, and cations, the relative energy is calculated for every 5° forward-backward motion within the range of -30° to $+30^\circ$. The nonsymmetric calculation ΔE - ϕ_3 plot of methoxyl group forward-backward motion is shown in Fig. 4(c). The ΔE values less than $50 \text{ kJ} \cdot \text{mol}^{-1}$ are observed for forward-backward motion of $-30^\circ < \phi_3 < +30^\circ$. Such motion energy barriers are obviously much smaller than those found in the pendulumlike cation motion mentioned above. Since the pendulumlike motion is frozen at around 156 K, the forward-backward motion of the methoxyl group should easily occur at room temperature and is frozen at lower temperature according to the motion calculation results. Interestingly, the solid-state NMR measurements also support this viewpoint; i.e., the terminal methoxyl group is dynamic until the temperature decreases to 125 K.

In conclusion, the paraelectric-ferroelectric phase transition at 153 K with an Aizu notation of $mmmFmm2$ in MOAP has been characterized. Electric hysteresis loop measurement shows a typical ferroelectric loop at 124 K with a spontaneous polarization of about $1.2 \mu\text{C} \cdot \text{cm}^{-2}$ and a remanent polarization of $0.9 \mu\text{C} \cdot \text{cm}^{-2}$. The motions of the supramolecular cation (4-methoxyanilinium)(18-crown-6) are frozen and the cation becomes ordered when the temperature decreases to 153 K as revealed by temperature-dependent solid-state NMR. However, the forward-backward motion of the methoxyl group of the cation is not frozen until the temperature below 126 K. The slowing down of pendulumlike swinging motion of 4-methoxyanilinium cation is the key to the origin of symmetric break, paraelectric-ferroelectric phase transition, strong dielectric anomaly, and ferroelectricity formation.

This work was supported by the National Natural Science Foundations of China (No. 20931002, No. 21101026, No. 21210005, and No. 21290172). The referees are greatly appreciated for their excellent suggestions to improve the quality of the manuscript. D-W.F., H-L.C., and S-H.L. contributed equally to this work.

*Corresponding author.
xiongrg@seu.edu.cn

[1] J.F. Scott and C.A.P. Dearaujo, *Science* **246**, 1400 (1989).

- [2] A. H. Moudden, D. E. Moncton, and J. D. Axe, *Phys. Rev. Lett.* **51**, 2390 (1983).
- [3] M. E. Lines and A. M. Glass, *Principles and Applications of Ferroelectrics and Related Materials* (Oxford University, New York, 2001).
- [4] K. Yoshimi, H. Seo, S. Ishibashi, and S. E. Brown, *Phys. Rev. Lett.* **108**, 096402 (2012).
- [5] D.-W. Fu, H.-L. Cai, Y. Liu, Q. Ye, W. Zhang, Y. Zhang, X.-Y. Chen, G. Giovannetti, M. Capone, J. Li *et al.*, *Science* **339**, 425 (2013).
- [6] D. A. Bonnelli, *Science* **339**, 401 (2013).
- [7] Y. Liu, Y. Zhang, M.-J. Chow, Q. N. Chen, and J. Li, *Phys. Rev. Lett.* **108**, 078103 (2012).
- [8] S. Horiuchi and Y. Tokura, *Nat. Mater.* **7**, 357 (2008).
- [9] J. N. Sherwood, *The Plastically Crystalline State* (Wiley, New York, 1979).
- [10] C. S. Vogelsberg and M. A. Garcia-Garibay, *Chem. Soc. Rev.* **41**, 1892 (2012).
- [11] T. Akutagawa, H. Koshinaka, D. Sato, S. Takeda, S.-I. Noro, H. Takahashi, R. Kumai, Y. Tokura, and T. Nakamura, *Nat. Mater.* **8**, 342 (2009).
- [12] A. S. Tayi *et al.*, *Nature (London)* **488**, 485 (2012).
- [13] F. Kagawa, S. Horiuchi, M. Tokunaga, J. Fujioka, and Y. Tokura, *Nat. Phys.* **6**, 169 (2010).
- [14] H.-L. Cai, W. Zhang, J.-Z. Ge, Y. Zhang, K. Awaga, T. Nakamura, and R.-G. Xiong, *Phys. Rev. Lett.* **107**, 147601 (2011).
- [15] D.-W. Fu, W. Zhang, H.-L. Cai, Y. Zhang, J.-Z. Ge, R.-G. Xiong, and S. D. Huang, *J. Am. Chem. Soc.* **133**, 12780 (2011).
- [16] W. Zhang, H. Y. Ye, and R. G. Xiong, *Coord. Chem. Rev.* **253**, 2980 (2009).
- [17] D.-W. Fu, W. Zhang, H.-L. Cai, Y. Zhang, J.-Z. Ge, R.-G. Xiong, S. D. Huang, and N. Takayoshi, *Angew. Chem., Int. Ed.* **50**, 11947 (2011).
- [18] D.-W. Fu, W. Zhang, H.-L. Cai, J.-Z. Ge, Y. Zhang, and R.-G. Xiong, *Adv. Mater.* **23**, 5658 (2011).
- [19] Y. Zhang, W. Zhang, S.-H. Li, Q. Ye, H.-L. Cai, F. Deng, R.-G. Xiong, and S. D. Huang, *J. Am. Chem. Soc.* **134**, 11044 (2012).
- [20] H.-L. Cai, D.-W. Fu, Y. Zhang, W. Zhang, and R.-G. Xiong, *Phys. Rev. Lett.* **109**, 169601 (2012).
- [21] See Supplemental Material at <http://link.aps.org/supplemental/10.1103/PhysRevLett.110.257601> for experimental details, crystallographic data and additional spectra.
- [22] F. Kagawa, S. Horiuchi, H. Matsui, R. Kumai, Y. Onose, T. Hasegawa, and Y. Tokura, *Phys. Rev. Lett.* **104**, 227602 (2010).
- [23] M. Szafranski, A. Katrusiak, and G. J. McIntyre, *Phys. Rev. Lett.* **89**, 215507 (2002).
- [24] S. D. Cady, C. Goodman, C. Tatko, W. F. DeGrado, and M. Hong, *J. Am. Chem. Soc.* **129**, 5719 (2007).
- [25] M. Hong, *J. Phys. Chem. B* **111**, 10340 (2007).
- [26] F. H. Hu, W. B. Luo, and M. Hong, *Science* **330**, 505 (2010).
- [27] F. Hu, K. Schmidt-Rohr, and M. Hong, *J. Am. Chem. Soc.* **134**, 3703 (2012).
- [28] M. J. Frisch *et al.*, *GAUSSIAN R03W* (Gaussian Inc., Pittsburgh, PA, 2003).